Enhanced OTFS using Channel Modulation

Nabarun Roy and A. Chockalingam
Department of ECE, Indian Institute of Science, Bangalore 560012

***Abstract*—Orthogonal time frequency space (OTFS) modulation provides robust communication in doubly-selective channels owing to its non-fading nature in the delay-Doppler (DD) domain. In this paper, for the first time in the literature, we propose a novel transmission scheme where the performance of OTFS is further enhanced through the use of channel modulation (a.k.a media-based modulation). In channel modulation (CM), radio frequency (RF) mirrors placed in the near-field of the transmit antenna are controlled by information bits, which create different channel fade realizations that form the CM alphabet. The proposed OTFS-CM scheme is shown to simultaneously offer the benefits of robustness to high-Doppler due to DD signal processing in OTFS and an additional SNR gain due to the improved distance properties of the signal set due to CM. For example, simulation results show that, at a bit error rate (BER) of 10^{-4}, the proposed OTFS-CM scheme achieves an SNR gain of about 1 to 4 dB compared to OTFS without CM, which is attributed to the enhanced distance profile of the OTFS-CM signal set. For the same reason, the SNR gain increases with increase in the dimensionality of the signal at the receiver and the number of RF mirrors.**

***Index Terms*—OTFS modulation, delay-Doppler domain, discrete Zak Transform, channel modulation, distance profile.**

I. Introduction

Future wireless communication systems are envisioned to support high data rate transmissions under diverse operational scenarios that include high-mobility scenarios. The dynamic nature of wireless channels in high-mobility conditions makes them doubly dispersive, with multipath fading causing time dispersion and Doppler shifts causing frequency dispersion. Multicarrier modulation schemes such as OFDM can mitigate the inter-symbol interference caused due to time dispersion, but they face performance degradation due to inter-carrier interference caused by loss of orthogonality among subcarriers due to Doppler shifts. Whereas, orthogonal time frequency space (OTFS) modulation, a modulation scheme in the delay-Doppler (DD) domain, offers robust performance in high-Doppler scenarios [1],[2].

Central to the OTFS modulation scheme is the multiplexing of information symbols in the DD domain and converting them to time domain for transmission (and vice versa at the receiver). In the first five years of OTFS research since its inception in 2017, this conversion was done in two steps, where the second step involves the legacy multicarrier (MC) modulation scheme [3]. Hence this scheme is referred to as MC-OTFS scheme. More recent research on OTFS has proposed the use of Zak transform approach to convert DD domain symbols to time domain in a single step [4],[5],[6]. This approach is referred to as Zak-OTFS. Compared to MC-OTFS approach, the Zak-OTFS approach has been shown to achieve better robustness to large Doppler spreads [5],[6]. Also, being attractive for practical implementation, a discrete Zak transform based OTFS (DZT-OTFS) approach has also been investigated recently [7],[8],[9]. In this paper, we propose a transmission scheme that further enhances the DZT-OTFS performance using channel modulation (a.k.a media-based modulation) [10],[11],[12].

This work was supported in part by the J. C. Bose National Fellowship, Department of Science and Technology, Government of India.

Channel modulation (CM) works on the principle that changing the radio frequency (RF) properties (e.g., any one or more of permittivity, permeability, resistivity) of the propagation environment close to the transmitter affects the end-to-end channel, and hence the magnitude and phase of the received signal [10]. Consequently, in a rich scattering environment, a small perturbation in the environment close to the transmitter will be augmented by many random reflections in the propagation path, resulting in an overall independent end-to-end channel realization. In CM, such near-field perturbations are created intentionally by switching ON/OFF RF elements placed near the transmitter (called RF mirrors) using information bits. Different combinations of information bits (called as mirror activation patterns) result in different channel realizations and these realizations are used as the CM alphabet to convey information bits. CM offers MIMO benefits at reduced RF hardware complexity/cost and improved performance due to good distance properties of the CM alphabet [11].

Inspired by the positive aspects of OTFS and CM, in this paper, we propose to enhance the performance of OTFS further by using CM, which has not been reported before. We call the proposed scheme as OTFS-CM scheme. The OTFS module considered in the proposed OTFS-CM scheme is the DZT-OTFS scheme in [8],[9]. The new contributions in the paper can be summarized as follows.

- First, we develop an end-to-end input-output relation for the proposed OTFS-CM scheme.
- We also derive an upper bound on the bit error rate (BER) performance of the proposed scheme under maximum likelihood (ML) detection. The upper bound is shown to be tight at high signal-to-noise ratios (SNRs).
- We further analyze the bit error performance through extensive simulations considering different system configuration settings using mimimum mean square error (MMSE) detection. Our simulation results show that 1) for the same bits per channel use (bpcu), the OTFS-CM scheme offers an SNR gain in the range 1 dB to 4 dB compared to OTFS without CM, 2) OTFS-CM performs better than OFDM with CM, and 3) the SNR gain in OTFS-CM compared to OTFS without CM increases with increase in the dimensionality of the received signal and the number of RF mirrors. The improved performance in the proposed scheme is attributed to the improved distance properties of the proposed OTFS-CM signal set.

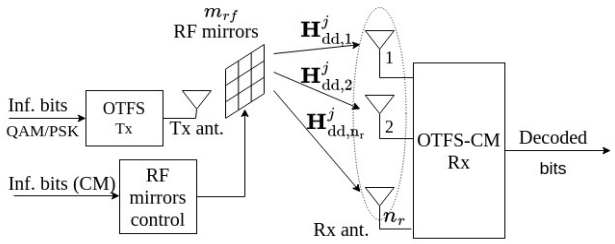

Fig. 1: Proposed OTFS-CM scheme.

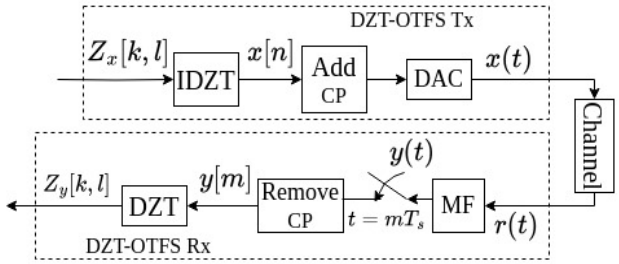

Fig. 2: Basic DZT-OTFS transceiver.

II. System model

The proposed OTFS scheme with channel modulation (OTFS-CM) is shown in Fig. 1. The transmitter uses a single transmit antenna and the receiver uses n_r receive antennas. Discrete Zak transform based OTFS (DZT-OTFS) waveform is used for multiplexing QAM/PSK symbols in the DD domain [8],[9]. Each OTFS frame consists of L delay bins and K Doppler bins, and KL information symbols drawn from an M-ary QAM/PSK alphabet $\mathbb{A}$ are mounted on the KL DD bins. In addition, channel modulation (a.k.a media based modulation [10],[11]) is used to convey additional information bits, using different fade realizations of the wireless channel as the channel modulation (CM) alphabet $\mathbb{B}$. To realize the CM alphabet, m_{rf} passive RF mirrors are placed in the near-field of the transmit antenna. These m_{rf} mirrors are controlled (i.e., switched ON/OFF) by m_{rf} bits in one OTFS frame duration. Different ON/OFF patterns of the mirrors result in different fade realizations at the receiver array, and the resulting n_r-length fade coefficient vectors form the CM alphabet $\mathbb{B}$. The number of fade realizations, i.e., the CM alphabet size, is $|\mathbb{B}| = 2^{m_{rf}}$. Therefore, the total number of bits sent in one OFTS frame is $KL\log_2|\mathbb{A}| + \log_2|\mathbb{B}|$, and the achieved rate in the proposed OTFS-CM scheme, in bits per channel use (bpcu), is given by $\eta_{\text{otfs-cm}} = \frac{1}{KL}(KL\log_2 M + m_{rf})$ bpcu. In the following subsection, we introduce the basic DZT-OTFS system model.

A. Basic DZT-OTFS system model

In this subsection, we present the basic DZT-OTFS system model and the input-output relation assuming $n_r = 1$ [8],[9], and subsequently extend this system model for the proposed OTFS-CM scheme with $n_r \geq 1$. The basic DZT-OTFS transceiver, assuming $n_r = 1$, is shown in Fig. 2. In DZT-OTFS, KL information symbols $\{Z_x[k,l] \in \mathbb{A}, k = 0,\cdots,K-1, l = 0,\cdots,L-1\}$ are multiplexed over a $K \times L$ DD grid, where K and L are the number of Doppler and delay bins, respectively. The $K \times L$ DD grid is defined as $\{(k\Delta\nu = \frac{k}{KLT_s}, l\Delta\tau = lT_s), k = 0,\cdots,K-1, l = 0,\cdots,L-1\}$, where $T_s = \frac{1}{B}$ is the symbol duration, B is the bandwidth available for communication, and $\Delta\tau = T_s$ and $\Delta\nu = \frac{1}{KLT_s}$ are the delay and Doppler resolutions, respectively. The information symbols multiplexed in the DD grid are converted into time domain using inverse DZT (IDZT) operation as

$$x[n] = \frac{1}{\sqrt{K}} \sum_{k=0}^{K-1} Z_x[k,(n)_L] e^{j2\pi \frac{\lfloor n/L \rfloor}{K}}, \tag{1}$$

where $\lfloor\cdot\rfloor$ and $(\cdot)_L$ denote the floor and modulo-L operators, respectively. A cyclic prefix (CP) of length N_{CP} is added to mitigate inter-frame interference. The sequence $x[n]$ is converted into a continuous time-domain signal $x(t)$ using transmit pulse $p_{tx}(t)$, $0 \leq t \leq T_s$, as

$$x(t) = \sum_{n=0}^{N+N_{\text{CP}}-1} x[(n-N_{\text{CP}})_N] p_{tx}(t-nT_s), \tag{2}$$

where $N = KL$ and $0 \leq t \leq (N+N_{\text{CP}})T_{\text{s}}$. The signal $x(t)$ passes through a doubly-selective channel with P resolvable DD paths, whose response is given by

$$h(\tau,\nu) = \sum_{i=1}^{P} h_i \delta(\tau-\tau_i)\delta(\nu-\nu_i), \tag{3}$$

where h_i, τ_i, and ν_i are the channel coefficient, delay, and Doppler associated with the ith path, respectively. The ith path's delay $\tau_i = (\alpha_i + a_i)T_{\text{s}}$, where α_i and $a_i \in (-0.5, 0.5]$ are the integer and fractional parts, respectively. Similarly, the ith path's Doppler $\nu_i = \frac{(\beta_i+b_i)}{KLT_{\text{s}}}$, where β_i and $b_i \in (-0.5, 0.5]$ are the integer and fractional parts, respectively. The received time-domain signal can then be expressed as

$$r(t) = \sum_{i=1}^{P} h_i \sum_{n=0}^{N+N_{\text{CP}}-1} x[(n-N_{\text{CP}}]p_{tx}(t-\tau_i-nT_s) \, e^{j2\pi\nu_i t} + w(t), \tag{4}$$

where $w(t)$ is the additive noise. The received signal $r(t)$ is matched filtered using the receive pulse $p_{rx}(t)$, by taking $p_{rx}(t) = p_{tx}(t)$. The matched filtered output $y(t)$ is sampled at $t = mT_s$, $m = 0, 1, \cdots, N+N_{\text{cp}}-1$, and the N_{cp} samples corresponding to the CP are discarded. The resulting time-domain received sequence $y[m]$ can be expressed as [8]

$$y[m] = \sum_{i=1}^{P} h_i e^{j2\pi\tau_i\nu_i} \sum_{n=0}^{N-1} x[n] e_i[n] g_i[m-n] + v[m], \tag{5}$$

where $m, n = 0, \cdots, N-1$, $v[m]$ is the additive noise sample at the output of the matched filter operation, $e_i[n] = e^{j2\pi\frac{k_i}{KL}n}$, $k_i = NT_s\nu_i$, and

$$g_i[n] = \frac{\sin(\pi(n-l_i)}{\pi(n-l_i)} \frac{\cos(\gamma\pi(n-l_i))}{1-(2\gamma(n-l_i))^2}, \quad l_i = \frac{\tau_i}{T_s},$$

where raised cosine (RC) pulses with roll-off factor γ are assumed for $p_{tx}(t)$ and $p_{rx}(t)$. The sequences $e_i[n]$ and $g_i[n]$ account for the effect of delay and Doppler of the ith path.

Equation (5) can be written as

$$y[m] = \sum_{i=1}^{P} h_i^{'} y_i[m] + v[m], \tag{6}$$

where

$$y_i[m] = \sum_{n=0}^{N-1} x[n] e_i[n] g_i[m-n], \tag{7}$$

and $h_i^{'} = h_i e^{j2\pi\tau_i\nu_i}$. The discrete time-domain received sequence in (6) is converted into DD domain using DZT operation as

$$Z_y[k,l] = \frac{1}{\sqrt{K}} \sum_{n=0}^{K-1} y[l+nL] e^{-j2\pi\frac{k}{K}n}. \tag{8}$$

The DD representation of (6) and (7) can be expressed as

$$Z_{y_i}[k,l] = \sum_{m=0}^{L-1} \sum_{n=0}^{K-1} Z_x[n,m] Z_{e_i}[k-n,m] Z_{g_i}[k,l-m], \tag{9}$$

and

$$Z_y[k,l] = \sum_{i=1}^{P} h_i^{'} Z_{y_i}[k,l] + Z_\nu[k,l], \tag{10}$$

where Z_{y_i}, Z_{e_i}, and Z_{g_i} denote the DZT of the sequences y_i, e_i, and g_i, respectively. The DD domain input-output relation in (10) can be obtained in the form

$$\mathbf{y}_{\text{dd}} = \mathbf{x}_{\text{dd}} \mathbf{H}_{\text{dd}} + \mathbf{v}_{\text{dd}}, \tag{11}$$

where $\mathbf{x}_{\text{dd}} \in \mathbb{A}^{1\times N}$ and $\mathbf{y}_{\text{dd}}, \mathbf{v}_{\text{dd}} \in \mathbb{C}^{1\times N}$ are vectorized column-wise such that $\mathbf{y}_{\text{dd}}(k+Kl) = Z_y[k,l]$, $\mathbf{x}_{\text{dd}}(k+Kl) = Z_x[k,l]$, $\mathbf{v}_{\text{dd}}(k+Kl) = Z_v[k,l]$ for $k = 0, \cdots, K-1$, $l = 0, \cdots, L-1$, and $\mathbf{H}_{\text{dd}} \in \mathbb{C}^{N\times N}$ is the effective DD domain channel matrix which can be written in the form

$$\mathbf{H}_{\text{dd}} = \sum_{i=1}^{P} h_i^{'} \mathbf{E}_i \mathbf{G}_i. \tag{12}$$

The matrix $\mathbf{E}_i$ in (12) is a block diagonal matrix with matrices $\{\mathbf{B}_u\}_{u=1}^{L}$ along the diagonal, where $\mathbf{B}_u$ is a $K \times K$ matrix whose jth row is $\mathbf{B}_u[j-1,:] = (Z_{e_i}[:,u-1])^T \mathbf{P}_K^{j-1}$, $u = 1, \cdots, L$, $j = 1, \cdots, K$, and $\mathbf{P}_K$ is a $K \times K$ basic circulant permutation matrix (BCPM) [13]. The matrix $\mathbf{G}_i$ is an $N \times N$ matrix given by $\mathbf{G}_i = \begin{bmatrix} \mathbf{A}\mathbf{Q}_1 \\ \vdots \\ \mathbf{A}\mathbf{Q}_L \end{bmatrix}$, where $\mathbf{A}$ is a $K \times N$ block matrix given by $\mathbf{A} = [\text{diag}\{Z_{g_i}[:,0]\}, \cdots, \text{diag}\{Z_{g_i}[:,L-1]\}]$ with $\text{diag}\{\mathbf{c}\}$ denoting a diagonal matrix with elements of $\mathbf{c}$, and $\mathbf{Q}_u = \mathbf{P}_L^{u-1} \otimes \mathbf{I}_K$ be an $N \times N$ matrix, where $\mathbf{P}_L$ is an $L \times L$ BCPM and $\otimes$ operator denotes Kronecker product.

III. Proposed OTFS-CM scheme and analysis

In this section, we extend the basic DZT-OTFS system model for $n_r = 1$ in (11) to the proposed OTFS-CM scheme for $n_r \geq 1$ and analyze it. In OTFS-CM, m_{rf} RF mirrors at the transmitter are controlled by m_{rf} bits in one OTFS frame time. A given realization of m_{rf} bits that control the m_{rf} mirrors is called a *mirror activation pattern* (MAP). There are $N_m = 2^{m_{rf}}$ possible MAPs. The fade coefficient realizations are different for different MAPs (due to MAP-induced RF mirror perturbations in the near-field of the transmit antenna getting augmented at the far-field receiver), while the delay and Doppler realizations remain same for all MAPs. The overall OTFS-CM effective channel matrix and the OTFS-CM signal set are obtained as follows.

OTFS-CM effective channel matrix: Let $\mathbf{H}_{\text{dd},i}^{j}$ denote the $N \times N$ effective channel matrix between the transmit antenna and the ith receive antenna ($i = 1, 2, \cdots, n_r$) corresponding to the jth MAP ($j = 1, 2, \cdots, N_m$), following the definition of the $\mathbf{H}_{\text{dd}}$ matrix in (12). Also, define a $N_m N \times N$ channel matrix $\mathbf{H}_{\text{dd},i}$ by staking matrices $\mathbf{H}_{\text{dd},i}^{j}$, $j = 1, \cdots, N_m$, as

$$\mathbf{H}_{\text{dd},i} = \begin{bmatrix} \mathbf{H}_{\text{dd},i}^{1} \\ \mathbf{H}_{\text{dd},i}^{2} \\ \vdots \\ \mathbf{H}_{\text{dd},i}^{N_m}. \end{bmatrix}. \tag{13}$$

Finally, stack the $\mathbf{H}_{\text{dd},i}$ matrices, $i = 1, 2, \cdots, n_r$, to define the overall $N_m N \times n_r N$ effective OTFS-CM channel matrix, denoted by $\bar{\mathbf{H}}_{\text{dd}}$, as

$$\bar{\mathbf{H}}_{\text{dd}} = [\mathbf{H}_{\text{dd},1}\ \mathbf{H}_{\text{dd},2}\ \cdots\ \mathbf{H}_{\text{dd},n_r}]. \tag{14}$$

OTFS-CM signal set: The basic DZT-OTFS transmit signal vector $\mathbf{x}_{\text{dd}}$ is a $1 \times N$ vector of s as defined in (11). The OTFS-CM transmit signal vector $\bar{\mathbf{x}}_{\text{dd}}$ is a $1 \times N_m N$ vector consisting of $(N_m - 1)$ zero vectors each of size $1 \times N$, and one basic DZT-OTFS transmit vector $\mathbf{x}_{\text{dd}}$ of size $1 \times N$. The location of the $\mathbf{x}_{\text{dd}}$ vector in the $\bar{\mathbf{x}}_{\text{dd}}$ vector is determined by the MAP index j, $j = 1, 2, \cdots, N_m$. The $\mathbf{x}_{\text{dd}}$ vector will carry N information symbols and the MAP index j is chosen based on m_{rf} information bits. Denoting the basic DZT-OTFS signal set as $\mathbb{S} = \mathbb{A}^{1\times N}$ and defining $\mathbb{S}_{\mathbf{0}} = \mathbb{S} \cup \{\mathbf{0}\}$, where $\mathbf{0}$ is $1 \times N$ zero vector, the OTFS-CM signal $\mathbb{S}_{\text{otfs-cm}}$ can be written as

$$\mathbb{S}_{\text{otfs-cm}} = \Big\{ \bar{\mathbf{s}} \in \mathbb{S}_{\mathbf{0}}^{N_m} : \bar{\mathbf{s}} = \big[\mathbf{0}\ \mathbf{0}\ \cdots \underbrace{\mathbf{s}}_{j\text{th position}} \cdots\ \mathbf{0}\ \mathbf{0}\big], \mathbf{s} \in \mathbb{S},\ j \in \{1, 2, \cdots, N_m\} \Big\}. \tag{15}$$

Using the OTFS-CM signal set definition in (15) and the overall effective channel matrix in (14), the end-to-end input-output relation in OTFS-CM can be written in the form

$$\bar{\mathbf{y}}_{\text{dd}} = \bar{\mathbf{x}}_{\text{dd}} \bar{\mathbf{H}}_{\text{dd}} + \bar{\mathbf{v}}_{\text{dd}}, \tag{16}$$

where $\bar{\mathbf{x}}_{\text{dd}} \in \mathbb{S}_{\text{otfs-cm}}$ is the OTFS-CM transmit vector, $\bar{\mathbf{y}}_{\text{dd}}$, $\bar{\mathbf{v}}_{\text{dd}} \in \mathbb{C}^{1\times n_r N}$ are the received vector and noise vector, respectively, and $\bar{\mathbf{H}}_{\text{dd}} \in \mathbb{C}^{N_m N \times n_r N}$ is the overall effective channel matrix.

OTFS-CM signal detection: The system model in (16) can be used to detect the OTFS-CM transmit vector (and hence the associated information bits) at the receiver. The optimum maximum-likelihood (ML) solution vector $\hat{\bar{\mathbf{x}}}_{\text{dd,ML}} \in \mathbb{S}_{\text{otfs-cm}}$ is given by

$$\hat{\bar{\mathbf{x}}}_{\text{dd,ML}} = \underset{\bar{\mathbf{x}}_{\text{dd}} \in \mathbb{S}_{\text{otfs-cm}}}{\text{argmin}} \ \|\bar{\mathbf{y}}_{\text{dd}} - \bar{\mathbf{x}}_{\text{dd}} \bar{\mathbf{H}}_{\text{dd}}\|^2. \tag{17}$$

The detected ML vector $\hat{\bar{\mathbf{x}}}_{\text{dd,ML}}$ is mapped back to the m_{rf} MAP index bits and the N information symbols in the OTFS frame. While the ML detection rule in (17) by exhaustive enumeration of $\bar{\mathbf{x}}_{\text{dd}}$ is feasible for small-sized frames (small values of N), it becomes infeasible for large frame sizes

due its exponential complexity. For large frame sizes, minimum mean square error (MMSE) detection with polynomial (cubic) complexity can be used. The MMSE solution vector $\tilde{\bar{\mathbf{x}}}_{\text{dd,MMSE}} \in \mathbb{C}^{1\times N_m N}$ is given by

$$\tilde{\bar{\mathbf{x}}}_{\text{dd,MMSE}} = \bar{\mathbf{y}}_{\text{dd}}\bar{\mathbf{H}}_{\text{dd}}^H(\bar{\mathbf{H}}_{\text{dd}}\bar{\mathbf{H}}_{\text{dd}}^H + \sigma^2\mathbf{I})^{-1}, \tag{18}$$

where $\mathbf{I}$ is a $N_m N \times N_m N$ identity matrix. From the MMSE solution vector $\tilde{\bar{\mathbf{x}}}_{\text{dd,MMSE}}$, the m_{rf} MAP index bits and the N information symbols in the OTFS frame are decoded as follows. A vector $\mathbf{v} \in \mathbb{R}^{1\times N_m}$ is defined such that its ith element is computed as

$$\mathbf{v}[i] = \sum_{q=(i-1)N+1}^{iN} |\tilde{\bar{\mathbf{x}}}_{\text{dd,MMSE}}[q]|^2, \quad i = 1, 2, \cdots, N_m. \tag{19}$$

The decoded MAP index $\hat{j}$ is obtained from vector $\mathbf{v}$ as

$$\hat{j} = \underset{i\in\{1,2,\cdots,N_m\}}{\text{argmax}} \mathbf{v}[i]. \tag{20}$$

The decoded MAP index $\hat{j}$ is mapped back to the corresponding m_{rf} bits. Now, define a vector $\mathbf{z} \in \mathbb{C}^{1\times N}$ such that is nth element is

$$\mathbf{z}[n] = \tilde{\bar{\mathbf{x}}}_{\text{dd,MMSE}}[(\hat{j}-1)N + n], \quad n = 1, 2, \cdots, N. \tag{21}$$

The nth decoded symbol in the OTFS frame is obtained as

$$\hat{\mathbf{x}}_{\text{dd}}[n] = \underset{x\in\mathbb{A}}{\text{argmin}} |x - \mathbf{z}[n]|^2, \quad n = 1, 2, \cdots, N. \tag{22}$$

A. Upper bound on the ML performance of OTFS-CM

The input-output relation for basic DZT-OTFS presented in (11) can be expressed in the form [9]

$$\mathbf{y}_{\text{dd}} = \mathbf{h}\mathbf{X} + \mathbf{v}_{\text{dd}}, \tag{23}$$

where $\mathbf{X} \in \mathbb{C}^{P\times N}$ can be expressed as

$$\mathbf{X} = (\mathbf{I}_P \otimes \mathbf{x}_{\text{dd}}) \begin{bmatrix} \mathbf{G}_1\mathbf{E}_1 \\ \vdots \\ \mathbf{G}_P\mathbf{E}_P \end{bmatrix}, \tag{24}$$

and

$$\mathbf{h} = [h_1^{'}\ h_2^{'} \cdots h_P^{'}]. \tag{25}$$

Likewise, the input-output relation for the OTFS-CM system model in (16) can be equivalently expressed as

$$\bar{\mathbf{y}}_{\text{dd}} = \bar{\mathbf{h}}\bar{\mathbf{X}} + \bar{\mathbf{v}}_{\text{dd}}, \tag{26}$$

where $\bar{\mathbf{h}}_{\text{dd}} = [\mathbf{h}_1^1 \cdots \mathbf{h}_i^j \cdots \mathbf{h}_{n_r}^{N_m}]$, $\mathbf{h}_i^j$ represents the equivalent fade coefficient vector for ith receive antenna and jth MAP in the form of the $\mathbf{h}$ vector in (25), and $\bar{\mathbf{X}}$ is a $PN_m n_r \times Nn_r$ matrix expressed as

$$\bar{\mathbf{X}} = \mathbf{I}_{n_r} \otimes \tilde{\mathbf{X}}_{\text{dd}}. \tag{27}$$

In (27), $\tilde{\mathbf{X}}_{\text{dd}}$ is a $PN_m \times N$ matrix obtained by stacking $\mathbf{X}$ (obtained in (24)) and $\mathbf{Z}_0$ (zero matrix of size $P \times N$) such that

$$\tilde{\mathbf{X}}_{\text{dd}} = \begin{bmatrix} \mathbf{Z}_0 \\ \vdots \\ \mathbf{X} \\ \vdots \\ \mathbf{Z}_0 \end{bmatrix} \leftarrow j\text{th position}, \tag{28}$$

where $\mathbf{X}$ occupies the jth position, i.e., the MAP index in $\tilde{\mathbf{X}}_{\text{dd}}$.The pairwise error probability (PEP) expression between two distinct transmitted signal vectors $\bar{\mathbf{x}}_{\text{dd}}^p$ and $\bar{\mathbf{x}}_{\text{dd}}^q$ can be obtained as

$$P(\bar{\mathbf{x}}_{\text{dd}}^p \to \bar{\mathbf{x}}_{\text{dd}}^q|\bar{\mathbf{h}}) = P(\|\bar{\mathbf{y}}_{\text{dd}} - \bar{\mathbf{h}}\bar{\mathbf{X}}_q\| < \|\bar{\mathbf{y}}_{\text{dd}} - \bar{\mathbf{h}}\bar{\mathbf{X}}_p\|) \tag{29}$$

$$= \text{Q}\left(\sqrt{\frac{\|\bar{\mathbf{h}}(\bar{\mathbf{X}}_q - \bar{\mathbf{X}}_p)\|^2}{2N_0}}\right), \tag{30}$$

where N_0 is the noise variance, and $\bar{\mathbf{X}}_p$ and $\bar{\mathbf{X}}_q$ are the equivalent matrix representations of $\bar{\mathbf{x}}_{\text{dd}}^p$ and $\bar{\mathbf{x}}_{\text{dd}}^q$, respectively. Using Chernoff bound, we can write

$$P(\bar{\mathbf{x}}_{\text{dd}}^p \to \bar{\mathbf{x}}_{\text{dd}}^q) \le \mathbb{E}_{\bar{\mathbf{h}}}\left\{\frac{1}{2}\exp\left(\frac{\|\bar{\mathbf{h}}(\bar{\mathbf{X}}_q - \bar{\mathbf{X}}_p)\|^2}{4N_0}\right)\right\}, \tag{31}$$

where $\mathbb{E}_{\bar{\mathbf{h}}}$ denotes the expectation operation over the random vector $\bar{\mathbf{h}}$. $\mathbf{h}_i^j$ is a unit energy random vector with its elements having identical and independent Gaussian distribution. Hence elements of $\mathbf{h}_i^j$ have zero mean and $1/P$ variance. Using SVD decomposition and taking expectation over $\bar{\mathbf{h}}$, (31) can be simplified as

$$P(\bar{\mathbf{x}}_{\text{dd}}^p \to \bar{\mathbf{x}}_{\text{dd}}^q) \le \frac{1}{2}\prod_{l=1}^{r}\frac{1}{1 + \frac{\lambda_{lpq}}{4PN_0}}, \tag{32}$$

where r is the rank of $(\bar{\mathbf{X}}_q - \bar{\mathbf{X}}_p)$ and λ_{lpq} is the lth eigen value of $(\bar{\mathbf{X}}_q - \bar{\mathbf{X}}_p)(\bar{\mathbf{X}}_q - \bar{\mathbf{X}}_p)^H$. Using union bound, an upper bound on the BER of OTFS-CM with ML detection can be obtained as

$$P_e \le \frac{1}{Q(KL\log_2 M + m_{rf})}\sum_{p=1}^{Q}\sum_{q=1,q\neq p}^{Q}\delta(\bar{\mathbf{x}}_{\text{dd}}^p, \bar{\mathbf{x}}_{\text{dd}}^q) \cdot P(\bar{\mathbf{x}}_{\text{dd}}^p \to \bar{\mathbf{x}}_{\text{dd}}^q), \tag{33}$$

where $\delta(\bar{\mathbf{x}}_{\text{dd}}^p, \bar{\mathbf{x}}_{\text{dd}}^q)$ is the hamming distance between $\bar{\mathbf{x}}_{\text{dd}}^p$ and $\bar{\mathbf{x}}_{\text{dd}}^q$ and $Q = N_m|\mathbb{A}|^{KL}$, where $|.|$ denotes the cardinality of the set.

B. Comparison of minimum distance of received OTFS and OTFS-CM signal sets

The relative performance of OTFS and OTFS-CM systems at high SNRs can be assessed by obtaining a metric based on the ratio of minimum distances of the received signal sets of these systems. Under same channel constraints (same number of paths, delays and Dopplers), $\mathbf{H}_{\text{dd}}$ in OTFS and $\bar{\mathbf{H}}_{\text{dd}}$ in OTFS-CM are generated. Let $\mathbb{S}_{\text{rx,otfs}}^{\text{H}}$ and $\mathbb{S}_{\text{rx,otfs-cm}}^{\text{H}}$ denote the received signal sets of OTFS and OTFS-CM, respectively, for a given channel realization in the absence of noise, and let $d_{\text{min,otfs}}^{\text{H}}$ and $d_{\text{min,otfs-cm}}^{\text{H}}$ represent the minimum distance between pairs of signal vectors in $\mathbb{S}_{\text{rx,otfs}}^{\text{H}}$ and $\mathbb{S}_{\text{rx,otfs-cm}}^{\text{H}}$, respectively, for the given channel realization, which can be expressed as

$$d_{\text{min,otfs}}^{\text{H}} = \min_{\mathbf{x}_{\text{dd}}^p, \mathbf{x}_{\text{dd}}^q \in \mathbb{S}_{\text{otfs}}} \|\mathbf{x}_{\text{dd}}^p\mathbf{H}_{\text{dd}} - \mathbf{x}_{\text{dd}}^q\mathbf{H}_{\text{dd}}\|^2, \tag{34}$$

and

$$d_{\text{min,otfs-cm}}^{\text{H}} = \min_{\bar{\mathbf{x}}_{\text{dd}}^p, \bar{\mathbf{x}}_{\text{dd}}^q \in \mathbb{S}_{\text{otfs-cm}}} \|\bar{\mathbf{x}}_{\text{dd}}^p\bar{\mathbf{H}}_{\text{dd}} - \bar{\mathbf{x}}_{\text{dd}}^q\bar{\mathbf{H}}_{\text{dd}}\|^2. \tag{35}$$

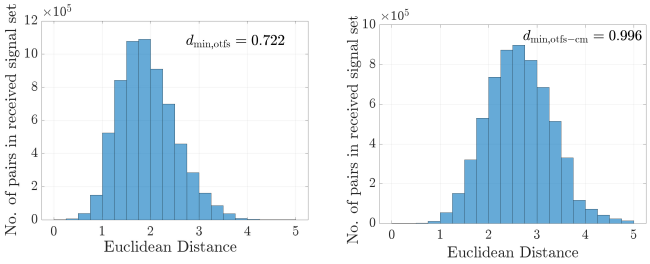

(a) OTFS without CM. (b) Proposed OTFS-CM.

Fig. 3: Distance distribution of signal vectors in the received signal set.

As the channel matrices in (34) and (35) are random, we use Monte Carlo simulation to find the average minimum distance over a large number of channel realizations. Let $d_{\text{min,otfs}}$ and $d_{\text{min,otfs-cm}}$ denote the average minimum distances which can be obtained as

$$d_{\text{min,otfs}} = \frac{1}{n_{\text{s}}} \sum_{i=1}^{n_{\text{s}}} d^{\text{H}}_{\text{min,otfs}}, \quad d_{\text{min,otfs-cm}} = \frac{1}{n_{\text{s}}} \sum_{i=1}^{n_{\text{s}}} d^{\text{H}}_{\text{min,otfs-cm}},$$

where n_{s} is the number of channel realizations in the simulation. The ratio of the average minimum distances gives the SNR gap between the BER performance of these systems at high SNRs with ML detection, and this SNR gap in dB is given by

$$\text{SNR}_{\text{gap}} = 20 \log \left(\frac{d_{\text{min,otfs-cm}}}{d_{\text{min,otfs}}} \right). \tag{36}$$

IV. Results and Discussions

In this section, we present the simulated BER performance of the proposed OTFS-CM scheme for different system settings and compare it with that of OTFS without CM and OFDM (without and with CM).

A. BER performance of OTFS-CM with ML detection

First, we consider the BER performance for small frame sizes for which ML detection is feasible. An OTFS system with $K = L = 2$ is considered with and without CM. A carrier frequency (f_c) of 4 GHz and ν_p of 3.75 kHz (hence, $\tau_p = \frac{1}{\nu_p} = 0.267$ ms) are considered. Hence, the delay resolution is $\Delta\tau = \frac{\tau_p}{L} = 0.1335$ ms and the Doppler resolution is $\Delta\nu = \frac{\nu_p}{K} = 1.875$ kHz. The channel is considered to have 4 paths (i.e., $P = 4$) with the DD profile in Table I.

TABLE I: DD profile of the channel.

P (no. of paths)	τ (delay)	ν (Doppler)
4	$[0,\ 0,\ 1,\ 1]\ \Delta\tau$	$[0,\ 1,\ 0,\ 1]\ \Delta\nu$

For the system without CM, the information symbols are chosen from 4-QAM alphabet and for the system with CM, the information symbols are chosen from BPSK alphabet with $m_{rf} = 4$ RF mirrors. This ensures that the achieved rate is 2 bits per channel use (bpcu) in both the systems.

1) Distance distribution of received signal sets: Figure 3 shows the distribution of the distance between pairs of signal points in the received signal set for both OTFS without and with CM for $n_r = 1$. The number of channel realizations taken in the simulation is $n_{\text{s}} = 500$. The average minimum distance $d_{\text{min,otfs}}$ and $d_{\text{min,otfs-cm}}$ obtained are 0.722 and 0.996, respectively. From (36), the SNR_{gap} at high SNRs can be calculated to be $20 \log \frac{0.996}{0.722} = 2.79$ dB. This improved distance profile of the OTFS-CM received signal set results in its better BER performance compared to OTFS without CM. This can be seen in Fig. 4 which shows the BER performance of OTFS-CM and OTFS without CM for $n_r = 1, 4$ and ML detection. Both simulated BER and upper bound on the BER are plotted, which shows the bound to be tight at high SNRs, validating the analysis.

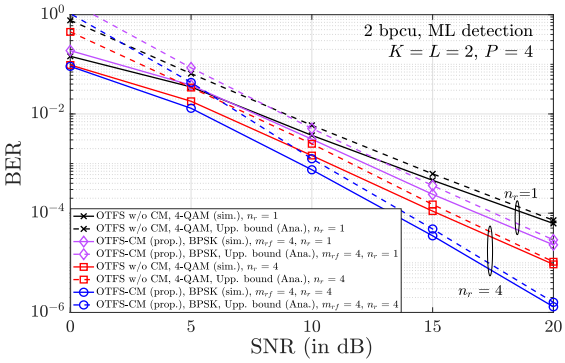

Fig. 4: BER performance of OTFS-CM and OTFS without CM as a function of SNR for $n_r = 1, 4$ under ML detection.

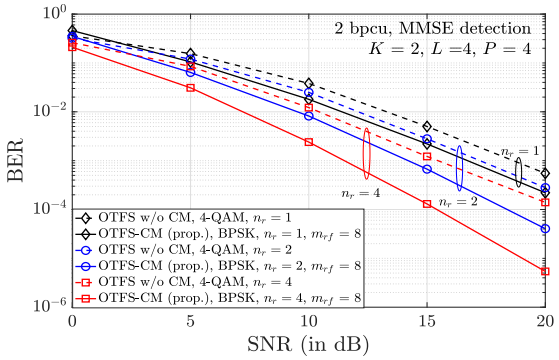

Fig. 5: BER performance of OTFS-CM and OTFS without CM as a function of SNR for $n_r = 1, 2, 4$ under MMSE detection.

B. BER performance of OTFS-CM with MMSE detection

Since ML detection is prohibitively complex, we have used MMSE detection for larger frame sizes. Figure 5 shows the BER performance of OTFS with and without CM under MMSE detection for $K = 2$, $L = 4$, and the (τ_p, ν_p) values considered in Fig. 4. The channel parameters in Table I are used. Information symbols are chosen from 4-QAM alphabet for OTFS without CM and BPSK alphabet for OTFS-CM. Eight RF mirrors $(m_{rf} = 8)$ are used in OTFS-CM to achieve the same rate of 2 bpcu in both the systems. From Fig. 5, it can be observed that OTFS-CM performs better than OTFS without CM illustrating the inherent strength of CM in terms of improving the distance properties of the received signal set. Also, for the same reason, increasing the number of receive antennas increases the performance gap between the two systems in favour of OTFS-CM.

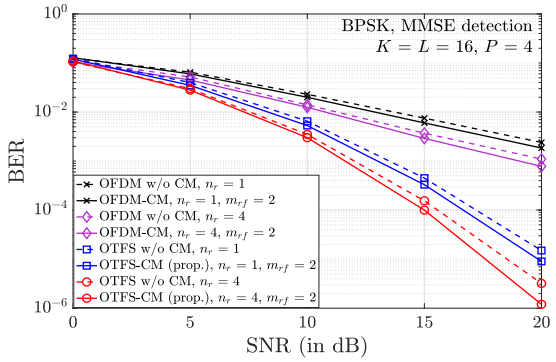

Fig. 6: BER performance of OTFS (with and without CM) and OFDM (with and without CM) as a function of SNR.

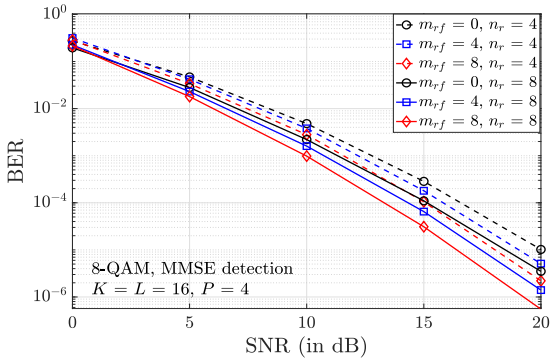

Fig. 7: BER performance of OTFS-CM as a function of SNR with 8-QAM for different values of m_{rf} and n_r.

C. BER performance of OTFS-CM and OFDM with CM

In Fig. 6, we present the BER performance of OTFS-CM in comparison with that of OFDM with CM. The following parameters are considered: bandwidth $B = 60\,\text{kHz}$ ($T_s = \frac{1}{B} = 16.67\,\mu\text{s}$), carrier frequency f_c = 4 GHz, and delay requirement $T = KLT_s = 4.27$ ms. Fixing $\nu_p = 3.75$ kHz gives $\tau_p = \frac{1}{\nu_p} = 0.267$ ms, $L = \left\lceil \frac{B}{\nu_p} \right\rceil = 16$, and $K = \left\lceil \frac{T}{\tau_p} \right\rceil = 16$. The number of RF mirrors (m_{rf}) is chosen to be 2 and the information symbols are chosen from BPSK alphabet. Hence, the rate with CM 1.0078 bpcu and the rate without CM is 1 bpcu. The channel is considered to have 4 paths ($P = 4$) with uniform power delay profile. For a given maximum delay $\tau_{\max}$ and maximum Doppler $\nu_{\max}$, the delay for the ith path is taken to be a random integer from uniformly sampled from $\left\{0, 1, \cdots, \text{round}\left(\frac{\tau_{\max}}{T_s}\right)\right\}$ and the ith path Doppler is taken as $\nu_{\max}\cos(\theta)$, where θ is uniformly distributed in $[-\pi, \pi]$. The $\tau_{\max}$ is taken to be $8T_s$ and $\nu_{\max}$ is taken to be 937 Hz. MMSE detection and $n_r = 1, 4$ are used. From Fig. 6, it can be seen that OTFS without CM outperforms OFDM without CM. Likewise, the proposed OTFS with CM significantly outperforms OFDM with CM.

D. Effect of m_{rf} and n_r on OTFS-CM performance

In Fig. 7, we show the effect of m_{rf} and n_r on OTFS-CM performance considering 8-QAM alphabet. The system configuration and channel parameters defined in Fig. 6 are used. The BER performance for $m_{rf} = 0, 4, 8$ and $n_r = 4, 8$ using MMSE detection are plotted. The achieved rates for $m_{rf} = 0, 4, 8$ are 3 bpcu, 3.015625 bpcu, and 3.03125 bpcu, respectively, which are roughly the same. It can be observed that with increasing number of RF mirrors and receive antennas, the performance of OTFS-CM improves due to increase in the dimensionality of the receive signal.

V. Conclusions

In this work, we proposed a new OTFS-CM scheme that enhanced the performance of the basic DZT-OTFS scheme in doubly-selective channels through the use of channel modulation. For the proposed OTFS-CM scheme, we derived a compact end-to-end DD domain input-output relation in a matrix-vector form, which we used to derive an upper bound on the BER with ML detection. The upper bound was found to be tight at high SNRs. We also carried out a detailed BER performance evaluation through simulations for large frame sizes and higher-order QAM using MMSE detection. Our simulation results showed an SNR gain of about 1 dB to 4 dB in favour of OTFS-CM compared to OTFS without CM. This improved performance is due to the improved distance properties of the received OTFS-CM signal set. Also, the OTFS-CM scheme performed better than OFDM with CM. In this work, we considered perfect knowledge of the channel. Channel estimation methods using machine learning techniques for OTFS-CM that exploit the predictability attribute of the ZAk-OTFS input-output relation [6] can be taken up as future work.

References

[1] R. Hadani et al., "Orthogonal time frequency space modulation," *Proc. IEEE WCNC'2017*, pp. 1-6, Mar. 2017.

[2] Y. Hong, T. Thaj, and E. Viterbo, *Delay-Doppler Communications: Principles and Applications,* Academic Press, 2022.

[3] "Best Readings in Orthogonal Time Frequency Space (OTFS) and Delay Doppler Signal Processing," June 2022. https://www.comsoc.org/publications/best-readings/orthogonal-time-frequency-space-otfs-and-delay-doppler-signal-processing

[4] S. K. Mohammed, "Derivation of OTFS modulation From first principles," *IEEE Trans. Veh. Tech.*, vol. 70, no. 8, pp. 7619-7636, Aug. 2021.

[5] S. K. Mohammed, R. Hadani, A. Chockalingam, and R. Calderbank, "OTFS - a mathematical foundation for communication and radar sensing in the delay-Doppler domain," *IEEE BITS the Information Theory Magazine*, vol. 2, no. 2, pp. 36-55, Nov. 2022.

[6] S. K. Mohammed, R. Hadani, A. Chockalingam, and R. Calderbank, "OTFS - predictability in the delay-Doppler domain and its value to communication and radar sensing," arXiv:2302.08705 [eess.SP] 17 Feb 2023. available https://arxiv.org/abs/2302.08705.

[7] A. J. E. M. Janssen, "The Zak transform: a signal transform for sampled time-continuous signals," *Philips J. Res.*, 43, pp. 23-69, 1988.

[8] F. Lampel, A. Avarado, and F. M. J. Willems, "On OTFS using the discrete Zak transform," *Proc. IEEE ICC'2022 Workshops*, pp. 729-734, May 2022.

[9] V. Yogesh, V. S. Bhat, S. R. Mattu, and A. Chockalingam, "On the bit error performance of OTFS modulation using discrete Zak transform," pp. 741-746, May 2023.

[10] A. K. Khandani, "Media-based modulation: a new approach to wireless transmission," *Proc. IEEE ISIT'2013*, pp. 3050-3054, Jul. 2013.

[11] Y. Naresh and A. Chockalingam, "On media-based modulation using RF mirrors," *IEEE Trans. Veh. Tech.*, vol. 66, no. 6, pp. 4967-4983, Jun. 2017.

[12] E. Basar and I. Altunbas, "Space-time channel modulation," *Proc. IEEE Trans. Veh. Tech.*, vol. 66, no. 8, pp. 7609-7614, Aug. 2017.

[13] R. Horn and C. Johnson, *Matrix Analysis*, Cambridge Univ. Press, 2013.